

UC San Diego

UC San Diego Previously Published Works

Title

Endoplasmic reticulum chaperone GRP78/BiP is critical for mutant Kras-driven lung tumorigenesis

Permalink

<https://escholarship.org/uc/item/992024sx>

Journal

Oncogene, 40(20)

ISSN

0950-9232

Authors

Rangel, Daisy Flores

Dubeau, Louis

Park, Ryan

et al.

Publication Date

2021-05-20

DOI

10.1038/s41388-021-01791-9

Peer reviewed



Published in final edited form as:

Oncogene. 2021 May ; 40(20): 3624–3632. doi:10.1038/s41388-021-01791-9.

Endoplasmic reticulum chaperone GRP78/BiP is critical for mutant *Kras*-driven lung tumorigenesis

Daisy Flores Rangel^{1,6}, Louis Dubeau^{2,6}, Ryan Park³, Priscilla Chan^{1,6}, Dat P. Ha^{1,6}, Mario A. Pulido^{4,6}, Daniel J. Mullen^{4,6}, Ivetta Vorobyova³, Beiyun Zhou⁵, Zea Borok^{1,5}, Ite A. Offringa^{1,4,6}, Amy S. Lee^{1,6,*}

¹Department of Biochemistry and Molecular Medicine, University of Southern California, Keck School of Medicine, Los Angeles, California, USA

²Department of Pathology, University of Southern California, Keck School of Medicine, Los Angeles, California, USA

³Department of Radiology, University of Southern California, Keck School of Medicine, Los Angeles, California, USA

⁴Department of Surgery, University of Southern California, Keck School of Medicine, Los Angeles, California, USA

⁵Department of Medicine, University of Southern California, Keck School of Medicine, Los Angeles, California, USA

⁶Norris Comprehensive Cancer Center, University of Southern California

Abstract

Lung cancer is the leading cause of cancer mortality worldwide and *KRAS* is the most commonly mutated gene in lung adenocarcinoma (LUAD). The 78-kDa glucose-regulated protein GRP78/BiP is a key endoplasmic reticulum (ER) chaperone protein and a major pro-survival effector of the unfolded protein response (UPR). Analysis of the Cancer Genome Atlas (TCGA) database and immunostain of patient tissues revealed that compared to normal lung, GRP78 expression is generally elevated in human lung cancers, including tumors bearing the *KRAS*^{G12D} mutation. To test the requirement of GRP78 in human lung oncogenesis, we generated mouse models containing floxed *Grp78* and *Kras* *Lox-Stop-Lox* *G12D* (*Kras*^{LSL-G12D}) alleles. Simultaneous activation of the *Kras*^{G12D} allele and knockout of the *Grp78* alleles were achieved in the whole lung or selectively in lung alveolar epithelial type 2 cells known to be precursors for adenomas which progress to LUAD. Here we report that GRP78 haploinsufficiency is sufficient to suppress *Kras*^{G12D}-mediated lung tumor progression and prolong survival. Furthermore, GRP78 knockdown in human lung cancer cell line A427 (*Kras*^{G12D/+}) leads to activation of UPR and

*Corresponding author: Amy S. Lee, Ph.D., Department of Biochemistry and Molecular Medicine, University of Southern California, Keck School of Medicine, USC Norris Comprehensive Cancer Center, 1441 Eastlake Avenue, Los Angeles, CA 90089. [Phone] 323-865-0507 [Fax] 323-865-0102 amylee@usc.edu.

Conflict of interest. The authors declare that they have no conflict of interest.

Ethical approval. All protocols for animal use and euthanasia were reviewed and approved by the University of Southern California Institutional Animal Care and Use Committee. Patient lung tissues were obtained in accordance with a protocol approved by the Institutional Review Board of the University of Southern California. Confirmed consent was obtained from all participants.

apoptotic markers and loss of cell viability. Our studies provide evidence that targeting GRP78 represents a novel therapeutic approach to suppress mutant *KRAS*-mediated lung tumorigenesis.

Introduction

Lung cancer is the leading cause of cancer mortality worldwide with limited therapeutic options (1). Non-small cell lung cancer (NSCLC) accounts for the majority (~85%) of all lung cancers and lung adenocarcinoma (LUAD) is the most common type of lung cancer in the United States. Activating mutations of the *KRAS* oncogene are found in one-quarter to one-half of human LUAD cases, resulting in constitutive activation of KRAS signaling (2, 3). *KRAS4B* is the predominant splice variant of *KRAS*, and hereafter will be referred to as *KRAS* (4). *KRAS* is a membrane-associated GTPase signaling protein that promotes proliferation and cell survival. Newly synthesized *KRAS* is cytosolic and inactive, and it undergoes a series of post-translational modifications at the cytosolic surface of the ER mediated by enzymes that are transmembrane ER proteins (5, 6). Thus, the ER is a major site for the maturation of *KRAS* and perturbation of ER homeostasis and dysregulated protein quality control could be detrimental to *KRAS*-driven LUAD.

The 78-kDa glucose regulated protein (GRP78), also referred to as BiP and encoded by the *HSPA5* gene, is an essential ER chaperone and a master regulator of ER functions (7, 8, 9). GRP78 exerts critical quality control of proteins processed in the ER impacting a wide range of human diseases including cancer (7, 10, 11). While GRP78 is primarily a luminal ER protein, upon stress, subfractions of GRP78 can be localized on the cell surface and other cellular compartments (12, 13). Through direct or indirect complex formation at the ER/cytosol interface, GRP78 regulates the activation of key proteins localized to the outer surface of the ER, such as caspase-7 and BCL interacting killer (BIK) (14, 15). Cancer cells, in response to intrinsic and extrinsic stress, often mount the adaptive unfolded protein response (UPR) (7, 10, 16). GRP78 is a key regulator of the UPR through complex formation with the transmembrane ER stress sensors and is a key pro-survival component of the UPR. GRP78 exhibits potent anti-apoptotic and pro-tumorigenic properties and is commonly over-expressed in human cancers (10, 17). In contrast to an earlier report (18), multiple recent studies have shown that lung cancer patients with LUAD expressing higher GRP78 levels had considerably shorter survival rates and worse prognosis compared to those with low levels (19–21). These findings suggest a potential role of GRP78 in promoting lung tumorigenesis, although the requirement of GRP78 in *KRAS*-driven lung cancer is not known.

Conditional expression of oncogenic *KRAS* in genetically modified mouse models utilizing the floxed mouse line *Kras lox-stop-lox G12D* (*Kras^{G12D}*) mimics human LUAD and has been used successfully to analyze lung tumor initiation and progression (2). To examine the role of GRP78 in mutant *Kras*-driven LUAD, we crossed the *Kras^{G12D}* mice with floxed *Grp78* (*Grp78^{fl/fl}*) mice (22). Simultaneous activation of the *Kras^{G12D}* allele and knockout of the *Grp78* alleles were achieved in the whole lung through intratracheal injection of adenovirus-Cre (adeno-Cre), or selectively in lung alveolar epithelial type 2 (AT2) cells known to be precursors for lung adenomas which progress to LUAD (23), by breeding with

an inducible human surfactant protein C (SPC)-Cre mouse model (24). Here we establish that GRP78 haploinsufficiency in these mouse models is sufficient to suppress *Kras*^{G12D}-driven LUAD and that knockdown of GRP78 in a human lung cancer cell line A427 (*Kras*^{G12D/+}) leads to activation of UPR and apoptotic markers and loss of cell viability.

Results

Suppression of Mutant *Kras*-driven Pulmonary Tumorigenesis by GRP78 Insufficiency.

Analysis of the Cancer Genome Atlas (TCGA) database showed that *GRP78* mRNA expression in human LUAD is significantly higher than in normal lungs (Fig. S1A). Further analysis of the LUAD tissues by mutation status of both *KRAS* and another commonly altered in LUAD, epidermal growth factor receptor (*EGFR*), revealed increased *GRP78* mRNA expression in LUAD tissues regardless of mutant or wild type status of *KRAS* or *EGFR*, in line with general upregulation of GRP78 in human tumors (Fig. S1B). Activating mutations in *KRAS* codon 12 are common in human LUAD (3) and all *KRAS* mutations in the TCGA analysis including the G12 type had increased *GRP78* mRNA expression over normal lung tissues (Fig. S1B). Furthermore, immunohistochemical (IHC) staining of patient tissues showed that compared to normal pulmonary alveoli and admixed non-neoplastic stromal cells, brown cytosolic staining of GRP78 is much more abundant in lung carcinomas bearing the *KRAS*^{G12D} mutation, as well as *KRAS* WT tumors (Fig. S1C).

In mice, the *Kras*^{G12D} mutation induces spontaneous LUAD (2). To investigate the requirement of GRP78 in LUAD development, we conditionally depleted GRP78 in the lungs of *Kras*^{G12D/+} mice containing either two floxed alleles of *Grp78* (*Grp78*^{f/f}) for homozygous deletion, or one floxed and one wild type allele (*Grp78*^{f/+}) for heterozygous deletion, with *Kras*^{G12D/+} mice containing two wild type alleles (*Grp78*^{+/+}) serving as control. These mice, referred to as *K78*^{f/f} (*Kras*^{G12D};*Grp78*^{f/f}), *K78*^{f/+} (*Kras*^{G12D};*Grp78*^{f/+}), *K78*^{+/+} (*Kras*^{G12D};*Grp78*^{+/+}) respectively, were generated as described in the breeding scheme (Fig. S2A). For the first mouse model, referred to as the adeno-Cre mice, the mice were subjected to intratracheal adeno-Cre administration to simultaneously activate the mutant *Kras* allele and delete the *Grp78* floxed allele (Fig. 1A). Polymerase chain reaction (PCR) of mouse tail and lung DNA confirmed the genotypes of the mice cohorts (Fig. 1B). Based on previous reports, three time points (12, 16, and 22 wk post-Cre-activation) were chosen for analysis and the lung tissues were subjected to immunohistochemistry (IHC).

Consistent with upregulation of GRP78 in human LUAD, strong immunostaining for GRP78 was detected in the tumor tissues of these mouse cohorts, as compared to the surrounding lung tissues (Fig. S3). As expected with Cre-mediated excision of the floxed *Grp78* allele, at all three time points, the staining intensity for GRP78 decreased by about 50% in the lungs of *K78*^{f/+} as compared to the *K78*^{+/+} mice, and was further decreased in *K78*^{f/f} mice (Fig. 1C and D and Fig. S4A and B). Correspondingly, the proliferation marker Ki67 showed a 45% and 80% decrease respectively in lung tissues of *K78*^{f/+} and in *K78*^{f/f} mice compared to *K78*^{+/+} mice (Fig. 1E and F).

Histological examination of tissue sections stained with hematoxylin and eosin (H&E) showed decreased lung tumor burden in the *K78*^{f/+} and even more so in *K78*^{f/f} mice

compared to $K78^{+/+}$ mice for all three time points analyzed (Fig. 2A and B). We next compared the frequency of pulmonary lesions [atypical adenomatous hyperplasia (AAH), adenoma, and LUAD] in each genotype by histological examination. Examples of each of these lesions as well as of adjacent normal tissues are shown in Fig. 2C. Consistent with the tumor burden measurements, pulmonary lesions appeared earlier in the $K78^{+/+}$ mice compared to the $K78^{f/+}$ and $K78^{f/f}$ mice. Lung lesions in $K78^{+/+}$ mice showed LUAD as early as 16 wk post-Cre-activation compared to 22 wk in $K78^{f/+}$ mice while LUAD was not observed in any of the $K78^{f/f}$ mice analyzed. Lungs of $K78^{f/f}$ mice were either histologically normal or showed AAH 12 wk post-intubation. In contrast, 50% of the $K78^{+/+}$ mice and 20% of the $K78^{f/+}$ mice showed adenomas at 12 wk post-intubation. Only adenomas were seen in the lungs of $K78^{f/f}$ mice at the 22 wk time point (Fig. 2D). Weight loss was detected in $K78^{+/+}$ mice starting at 18 wk, which was not observed in the $K78^{f/+}$ or $K78^{f/f}$ mice (Fig. S2B).

These histological observations were further confirmed through imaging of the mouse lungs at 12, 16, and 22 wk. Contrast-enhanced, computerized tomography (CT) segmentation was aided by ^{18}F -fluorodeoxyglucose (FDG) positron emission tomography (PET)/CT signal to determine the progression of lung tumors in the three genotypes. $K78^{+/+}$ and $K78^{f/+}$, but not $K78^{f/f}$ mouse, showed FDG uptake in the lung regions (Fig. 3A). Consistent with detection of LUAD in the $K78^{+/+}$ mouse, PET scans revealed earlier and higher FDG uptake in the $K78^{+/+}$ mouse compared to the $K78^{f/+}$ mouse. Three-dimensional visualization of FDG corroborated contrast-enhanced CT and confirmed that the tumor burden was highest in the $K78^{+/+}$ mouse, which was reduced in the $K78^{f/+}$ mouse and hardly detectable in the $K78^{f/f}$ mouse at all three time points (Fig. 3B).

GRP78 Haploinsufficiency in Lung Alveolar Epithelial Type 2 Cells is Sufficient to Halt Lung Tumor Progression and Prolong Survival.

The presence of oncogenic $Kras^{G12D}$ in lung AT2 cells leads to multifocal clonal adenomas progressing to LUAD (23). Thus, in our second approach, referred to below as the SPC-Cre model, we tested the effect of an inducible conditional knockout of $Grp78$ targeted to AT2 cells carrying a $Kras^{G12D}$ mutation to induce lung tumorigenesis. This approach utilized a previously described SPC-CreER^{T2} construct that includes the SPC promoter enabling Cre expression in AT2 cells and the estrogen receptor portion allowing inducibility by tamoxifen (tam) (24). The breeding scheme to generate mouse cohorts carrying a single copy of SPC-CreER^{T2}, a single copy of the $Kras^{G12D}$ knock-in allele, and either wild type ($CK78^{+/+}$), 1 or 2 copies of the floxed $Grp78$ allele ($CK78^{f/+}$ and $CK78^{f/f}$, respectively) is summarized in Fig. S5A. At 10 wk of age, mice were injected with tam and lungs were genotyped and examined at various time points (Fig. 4A and B). We noted that the mortality of the $CK78^{+/+}$ mice started at around 3 wk post-tam injection and that none of these mice survived more than 8 wk post-injection, whereas $CK78^{f/+}$ and $CK78^{f/f}$ mice survived over 30 wk post injection (Fig. 4C). Necropsy examination of the $CK78^{+/+}$ mice revealed that the abnormalities were confined to the lungs which showed multiple tumor nodules; in comparison, lungs and other organs of tam-injected $CK78^{+/+}$ mice carrying only the SPC-Cre allele appeared to be normal, consistent with the notion that tumorigenesis observed in the $CK78^{+/+}$ mice was dependent on mutant $Kras$ (Fig. S5B).

Representative GRP78 immunostains and histological images of the lung sections of the three genotypes are shown in Fig. 4D. For example, *CK78^{+/+}* mice exhibited robust GRP78 staining of adenomas and LUAD at 8 wk following tam injection (Fig. 4D–F). *CK78^{f/+}* mice showed reduction of GRP78 expression, which was further decreased in *CK78^{f/f}* mice (Fig. 4E). Tumor prevalence and grade were much reduced in both genotypes, with *CK78^{f/+}* mice showing predominantly adenoma while *CK78^{f/f}* lesions were primarily AAH even at 12 wk after tam injection (Fig. 4D and F). In comparison, the lung cells of the *C78^{f/f}* mice carrying only the *SPC-Cre* and *Grp78* floxed alleles appeared normal at 12 wk after tam injection (Fig. S5C). Similar to the adeno-Cre model, weight loss was observed in *CK78^{+/+}* mice but not in the *CK78^{f/+}* and *CK78^{f/f}* mice (Fig. S5D), and the staining intensity of GRP78 was higher in the tumor compared to surrounding lung tissues (Fig. S6). Collectively, these results indicate that GRP78 haploinsufficiency in AT2 cells is sufficient to suppress mutant *Kras*-driven lung tumorigenesis and prolong survival.

Towards understanding potential mechanisms whereby GRP78 deficiency impedes lung tumorigenesis, we utilized the human lung cancer cell line A427, which harbors the same *KRAS^{G12D}* mutation as our mouse models and offers an experimental system for biochemical analysis. Consistent with GRP78 being a key regulator of the UPR, knockdown of GRP78 by siRNA led to UPR activation (Fig. 4G), as exemplified by upregulation of phosphorylated eIF2 α (p-eIF2 α), which is a downstream effector of the ER stress sensor protein kinase R-like ER kinase (PERK), as well as the splicing of X-box binding protein 1 (XBP-1) mRNA, a downstream effector of the ER stress sensor inositol-requiring enzyme 1 α (IRE1 α). The activation of apoptotic markers, including C/EBP homologous protein (CHOP), which is downstream of PERK activation, cleaved caspase-7 (c-C7), and cleaved poly (ADP-ribose) polymerase (PARP) (c-PARP), were also detected, corresponding with decrease in cell viability (Fig. 4G).

Discussion

Curbing mutant KRAS-driven tumorigenesis remains elusive as clinical responses to most inhibitors can be relatively short-lived due to compensatory mechanisms leading to acquired resistance. Here, we discovered a new approach to suppress KRAS oncogenesis by targeting a critical ER chaperone, GRP78. Upregulation of GRP78 is generally observed in human tumors due to intrinsic and extrinsic stress (10). This study further reveals that *GRP78* mRNA and protein levels are upregulated in human LUAD bearing *KRAS* mutations, including the G12D mutation used in our mouse models. This, coupled with our finding that knockdown of GRP78 in the human lung cancer A427 cells bearing the *KRAS^{G12D}* mutation reduced their viability, in agreement with similar observations in A549 cells bearing *KRAS^{G12S}* mutation (17), suggests GRP78 could be a novel therapeutic target for LUAD, including those harboring *KRAS* mutations. Tissue-specific ablation of GRP78 using genetically engineered mouse models established the requirement of GRP78 in *Pten*-null driven cancers and PI3K/AKT signaling (10, 22, 25). GRP78 haploinsufficiency suppresses acinar-to-ductal metaplasia, proliferative signaling and mutant *Kras*-driven pancreatic tumorigenesis in mice (26). Based on the established utility of the *Kras^{G12D}* mouse model for monitoring lung cancer initiation and progression (2), here, we created new mouse models where heterozygous activation of mutant *Kras^{G12D}* is coupled with mono- or

Materials and Methods

Mouse models, Cre activation and tissue processing, ¹⁸F-FDG PET/CT imaging, tissue staining, quantitation of tumor burden, grading of pulmonary tumors, cell culture, Western blot analysis, cell viability assay, gene expression data, human specimens and immunostains as well as statistical analysis can be found in Supplemental Information.

Supplementary Material

Refer to Web version on PubMed Central for supplementary material.

Acknowledgements

We thank Hal Chapman for the SPC-Cre mice, Peter Conti and Jennifer Choi for assistance with PET/CT, and Jorge Nieva and Robert Hsu for tumor samples. The work was supported by NIH grants R01 CA027607 and the Judy and Larry Freeman Chair (A.S. Lee), NIH Diversity Supplements (D. F. Rangel), the Hastings Foundation (B. Zhou, Z. Borok) and NIH grant R35 HL135747 and Ralph Edgington Chair (Z. Borok). We thank the USC Norris Comprehensive Cancer Translational Pathology Core and the USC Molecular Imaging Center (supported by P30 CA014089, 1S10OD012371 and 1S10OD18500) for technical assistance.

References

1. Torre LA, Bray F, Siegel RL, Ferlay J, Lortet-Tieulent J, Jemal A. Global cancer statistics, 2012. *CA Cancer J Clin.* 2015; 65: 87–108. [PubMed: 25651787]
2. Jackson EL, Willis N, Mercer K, Bronson RT, Crowley D, Montoya R, et al. Analysis of lung tumor initiation and progression using conditional expression of oncogenic K-ras. *Genes Dev.* 2001; 15: 3243–3248. [PubMed: 11751630]
3. Cancer Genome Atlas Research Network, Comprehensive molecular profiling of lung adenocarcinoma. *Nature.* 2014; 511: 543–550. [PubMed: 25079552]
4. Hancock JF, Magee AI, Childs JE, Marshall CJ. All ras proteins are polyisoprenylated but only some are palmitoylated. *Cell.* 1989; 57: 1167–1177. [PubMed: 2661017]
5. Hancock JF, Paterson H, Marshall CJ. A polybasic domain or palmitoylation is required in addition to the CAAX motif to localize p21ras to the plasma membrane. *Cell.* 1990; 63:133–139. [PubMed: 2208277]
6. Dai Q, Choy E, Chiu V, Romano J, Slivka SR, Steitz SA, et al. Mammalian prenylcysteine carboxyl methyltransferase is in the endoplasmic reticulum. *J Biol Chem.* 1998; 273:15030–15034. [PubMed: 9614111]
7. Luo B, Lee AS. The critical roles of endoplasmic reticulum chaperones and unfolded protein response in tumorigenesis and anticancer therapies. *Oncogene.* 2013; 32: 805–818 [PubMed: 22508478]
8. Ni M, Lee AS. ER chaperones in mammalian development and human diseases. *FEBS Lett.* 2007; 581: 3641–3651. [PubMed: 17481612]
9. Pobre KFR, Poet GJ, Hendershot LM. The endoplasmic reticulum (ER) chaperone BiP is a master regulator of ER functions: Getting by with a little help from ERdj friends. *J Biol Chem.* 2019; 294: 2098–2108. [PubMed: 30563838]
10. Lee AS. Glucose-regulated proteins in cancer: molecular mechanisms and therapeutic potential. *Nat Rev Cancer.* 2014; 14: 263–276. [PubMed: 24658275]
11. Wang M, Kaufman RJ. The impact of the endoplasmic reticulum protein-folding environment on cancer development. *Nature Rev Cancer.* 2014; 14: 581–597. [PubMed: 25145482]
12. Zhang Y, Liu R, Ni M, Gill P, Lee AS. Cell surface relocalization of the endoplasmic reticulum chaperone and unfolded protein response regulator GRP78/BiP. *J Biol Chem.* 2010; 285: 15065–15075. [PubMed: 20208072]

13. Ni M, Zhang Y, Lee AS. Beyond the endoplasmic reticulum: atypical GRP78 in cell viability, signalling and therapeutic targeting. *Biochem J.* 2011; 434: 181–188. [PubMed: 21309747]
14. Reddy RK, Mao C, Baumeister P, Austin RC, Kaufman RJ, Lee AS. Endoplasmic reticulum chaperone protein GRP78 protects cells from apoptosis induced by topoisomerase inhibitors: role of ATP binding site in suppression of caspase-7 activation. *J Biol Chem.* 2003; 278: 20915–20924. [PubMed: 12665508]
15. Fu Y, Li J, Lee AS. GRP78/BiP inhibits endoplasmic reticulum BIK and protects human breast cancer cells against estrogen starvation-induced apoptosis. *Cancer Res.* 2007; 67:3734–3740. [PubMed: 17440086]
16. Rutkowski DT, Arnold SM, Miller CN, Wu J, Li J, Gunnison KM, et al. Adaptation to ER stress is mediated by differential stabilities of pro-survival and pro-apoptotic mRNAs and proteins. *PLoS Biol.* 2006; 4: doi:10.1371/journal.pbio.0040374.
17. Chae YC, Caino MC, Lisanti S, Ghosh JC, Dohi T, Danial NN, et al. Control of tumor bioenergetics and survival stress signaling by mitochondrial HSP90s. *Cancer Cell.* 2012; 22: 331–344. [PubMed: 22975376]
18. Uramoto H, Uchiumi T, Izumi H, Kohno K, Oyama T, Sugio K, et al. A new mechanism for primary resistance to gefitinib in lung adenocarcinoma: the role of a novel G796A mutation in exon 20 of EGFR. *Anticancer Res.* 2007; 27: 2297–2303. [PubMed: 17695517]
19. Ma X, Guo W, Yang S, Zhu X, Xiang J, Li H. Serum GRP78 as a tumor marker and its prognostic significance in non-small cell lung cancers: a retrospective study. *Dis Markers.* 2015; doi:10.1155/2015/814670.
20. Kwon D, Koh J, Kim S, Go H, Min HS, Kim YA, et al. Overexpression of endoplasmic reticulum stress-related proteins, XBP1s and GRP78, predicts poor prognosis in pulmonary adenocarcinoma. *Lung Cancer.* 2018; 122: 131–137. [PubMed: 30032821]
21. Imai H, Kaira K, Minato K. Clinical significance of post-progression survival in lung cancer. *Thorac Cancer.* 2017; 8: 379–386. [PubMed: 28627767]
22. Fu Y, Wey S, Wang M, Ye R, Liao CP, Roy-Burman P, et al. Pten null prostate tumorigenesis and AKT activation are blocked by targeted knockout of ER chaperone GRP78/BiP in prostate epithelium. *Proc Natl Acad Sci U S A.* 2008; 105: 19444–19449. [PubMed: 19033462]
23. Desai TJ, Brownfield DG, Krasnow MA. Alveolar progenitor and stem cells in lung development, renewal and cancer. *Nature.* 2014; 507: 190–194. [PubMed: 24499815]
24. Chapman HA, Li X, Alexander JP, Brumwell A, Lorizio W, Tan K, et al. Integrin alpha6beta4 identifies an adult distal lung epithelial population with regenerative potential in mice. *J Clin Invest.* 2011; 121: 2855–2862. [PubMed: 21701069]
25. Wey S, Luo S, Tseng CC, Ni M, Zhou H, Fu Y, et al. Inducible knockout of GRP78/BiP in the hematopoietic system suppresses Pten-null leukemogenesis and AKT oncogenic signaling. *Blood.* 2012; 119: 817–825. [PubMed: 21937694]
26. Shen J, Ha DP, Zhu G, Rangel DF, Kobiela A, Gill PS, et al. GRP78 haploinsufficiency suppresses acinar-to-ductal metaplasia, signaling, and mutant Kras-driven pancreatic tumorigenesis in mice. *Proc Natl Acad Sci U S A.* 2017; 114: E4020–E4029. [PubMed: 28461470]
27. Du T, Li H, Fan Y, Yuan L, Guo X, Zhu Q, et al. The deubiquitylase OTUD3 stabilizes GRP78 and promotes lung tumorigenesis. *Nat Commun.* 2019; 10: 2914. [PubMed: 31266968]
28. Ye R, Jung DY, Jun JY, Li J, Luo S, Ko HJ, et al. Grp78 heterozygosity promotes adaptive unfolded protein response and attenuates diet-induced obesity and insulin resistance. *Diabetes.* 2010; 59: 6–16. [PubMed: 19808896]
29. Lee AS, Brandhorst S, Rangel DF, Navarrete G, Cohen P, Longo VD, et al. Effects of prolonged GRP78 haploinsufficiency on organ homeostasis, behavior, cancer and chemotoxic resistance in aged mice. *Sci Rep.* 2017; 7: 40919. [PubMed: 28145503]
30. Zhang X, He Z, Xiang L, Li L, Zhang H, Lin F, et al. Codelivery of GRP78 siRNA and docetaxel via RGD-PEG-DSPE/DOPA/CaP nanoparticles for the treatment of castration-resistant prostate cancer. *Drug Des Devel Ther.* 2019; 13: 1357–1372.
31. Cerezo M, Lehraiki A, Millet A, Rouaud F, Plaisant M, Jaune E, et al. Compounds triggering ER stress exert anti-melanoma effects and overcome BRAF inhibitor resistance. *Cancer Cell.* 2016; 29: 805–819. [PubMed: 27238082]

32. Bakewell SJ, Rangel DF, Ha DP, Sethuraman J, Crouse R, Hadley E, et al. Suppression of stress induction of the 78-kilodalton glucose regulated protein (GRP78) in cancer by IT-139, an anti-tumor ruthenium small molecule inhibitor. *Oncotarget*. 2018; 9: 29698–29714. [PubMed: 30038714]
33. Burris HA, Bakewell S, Bendell JC, Infante J, Jones SF, Spigel DR, et al. Safety and activity of IT-139, a ruthenium-based compound, in patients with advanced solid tumours: a first-in-human, open-label, dose-escalation phase I study with expansion cohort. *ESMO Open*. 2016; 1: dx.doi.10.1136/esmoopen-2016-000154.
34. Gifford JB, Huang W, Zeleniak AE, Hindoyan A, Wu H, Donahue TR, et al. Expression of GRP78, Master Regulator of the Unfolded Protein Response, Increases Chemoresistance in Pancreatic Ductal Adenocarcinoma. *Mol Cancer Ther*. 2016; 15: 1043–1052. [PubMed: 26939701]
35. Lizardo MM, Morrow JJ, Miller TE, Hong ES, Ren L, Mendoza A, et al. Upregulation of Glucose-Regulated Protein 78 in metastatic cancer cells is necessary for lung metastasis progression. *Neoplasia*. 2016; 18: 699–710. [PubMed: 27973325]
36. Denoyelle C, Abou-Rjaily G, Bezrookove V, Verhaegen M, Johnson TM, Fullen DR, et al. Anti-oncogenic role of the endoplasmic reticulum differentially activated by mutations in the MAPK pathway. *Nat Cell Biol*. 2006; 8: 1053–1063. [PubMed: 16964246]
37. De Raedt T, Walton Z, Yecies JL, Li D, Chen Y, Malone CF, et al. Exploiting cancer cell vulnerabilities to develop a combination therapy for ras-driven tumors. *Cancer Cell*. 2011; 3: 400–413.

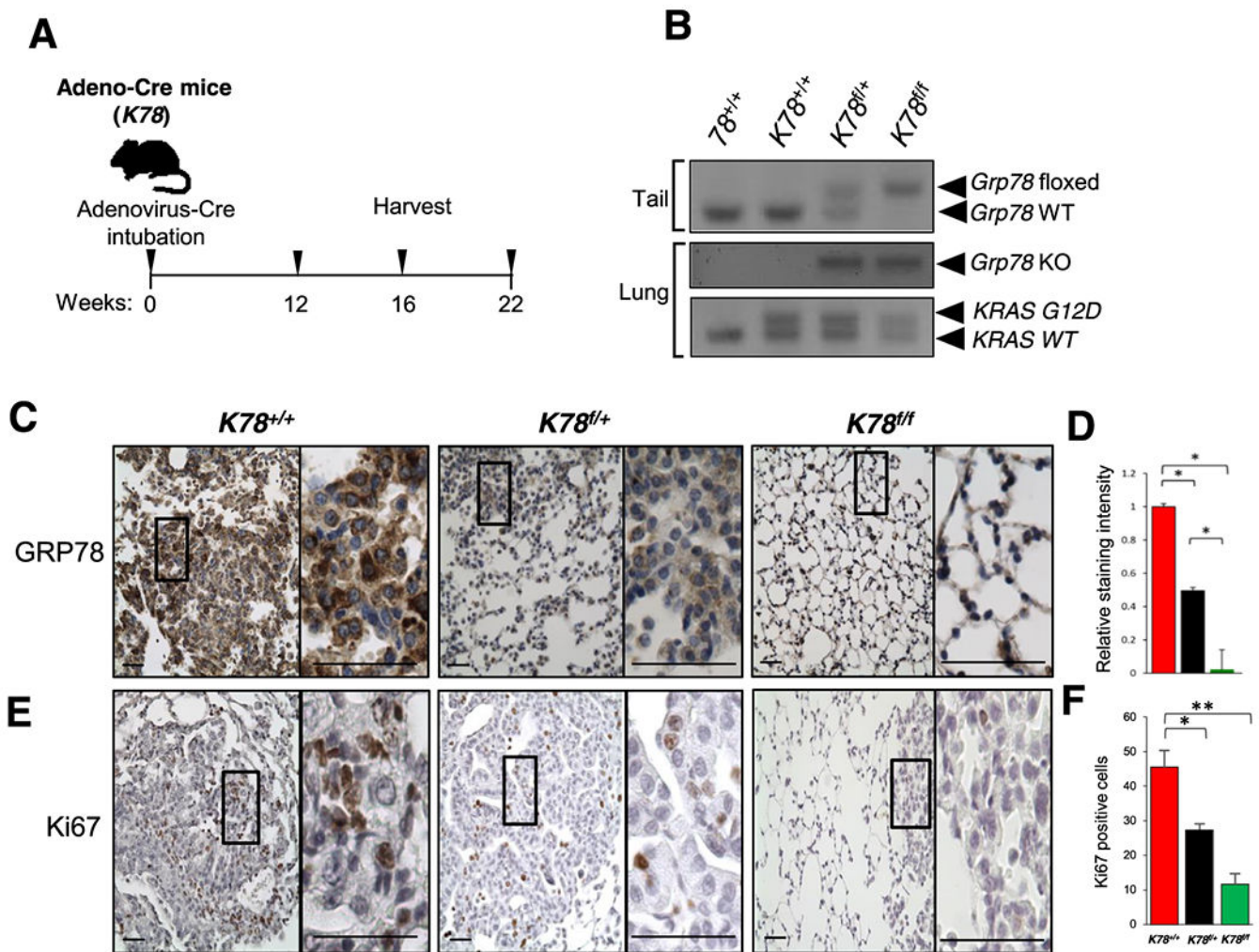


Fig. 1. Characterization of the adenovirus-Cre mouse model.

a Timeline of mice analysis. 10 wk old adult mice were intubated with adenovirus-Cre (adeno-Cre) and the lungs were harvested and processed for analysis at 12, 16 and 22 wk post adeno-Cre treatment. **b** Representative genotyping results of the adeno-Cre mice using DNA extracted from tail (top panel) and from lung (bottom two panels) after Cre treatment. **c** Immunohistochemistry (IHC) of GRP78 in lungs of the indicated genotypes 12 wk post adeno-Cre treatment by intratracheal intubation (Scale bar: 100 μ m). Enlarged views of the boxed area are shown on the right (Scale bar: 100 μ m). **d** Quantitation of GRP78 staining from (c). The values represent the average staining of the sampled area \pm s.e., * p <0.05. Number of images that were randomly chosen to be quantified are the following *K78^{+/+}* (n=20), *K78^{fl/+}* (n=20) and *K78^{fl/fl}* (n=20). At least three to four mice were analyzed per genotype. **e** Representative immunostains for Ki67 in lungs of mice of the indicated genotypes 22 wk post adeno-Cre treatment. Magnifications same as (c). **f** Quantitation of Ki67 positive cells using 5 random high-power fields of lung tissues 22 wk after adeno-Cre treatment from (e). Data are presented as mean \pm s.e., * p <0.05 and ** p <0.01.

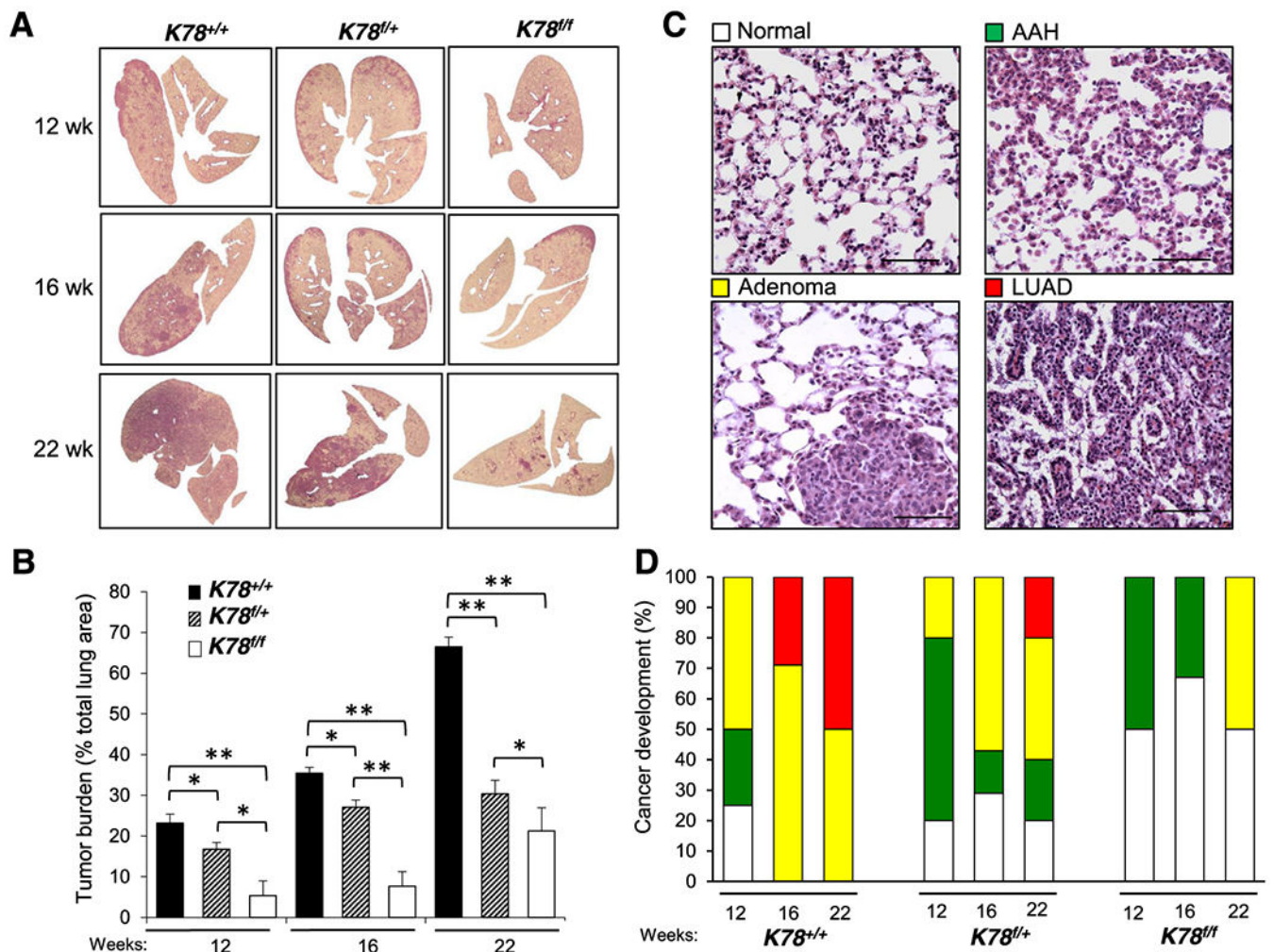


Fig. 2. Comparative analysis of the lungs of $K78^{+/+}$, $K78^{f/+}$ and $K78^{f/f}$ mice following adenovirus-Cre treatment.

a Panels showing cross sections of whole lungs from mice of the indicated genotypes at 12, 16, or 22 wk post adenovirus-Cre injection. **b** Quantitation of tumor burden for the $K78^{+/+}$, $K78^{f/+}$, $K78^{f/f}$ mice at 12 wk (n=9, 8 and 9, respectively), 16 wk (n=8, 9 and 11, respectively), and 22 wk (n=9, 8 and 8, respectively). The *p*-values compare the two genotypes under each bracket. Data are presented as mean \pm s.e., **p*<0.05 and ***p*<0.01. **c** Panels show representative examples of hematoxylin and eosin (H&E) staining of lung tissues exhibiting normal morphology, atypical adenomatous hyperplasia (AAH), adenoma, or adenocarcinoma (LUAD) (Scale bar: 200 μ m). **d** Quantitation of the histological grades of lungs of the mice of the indicated genotypes at the indicated time points. The number of mice analyzed was the same as in (b).

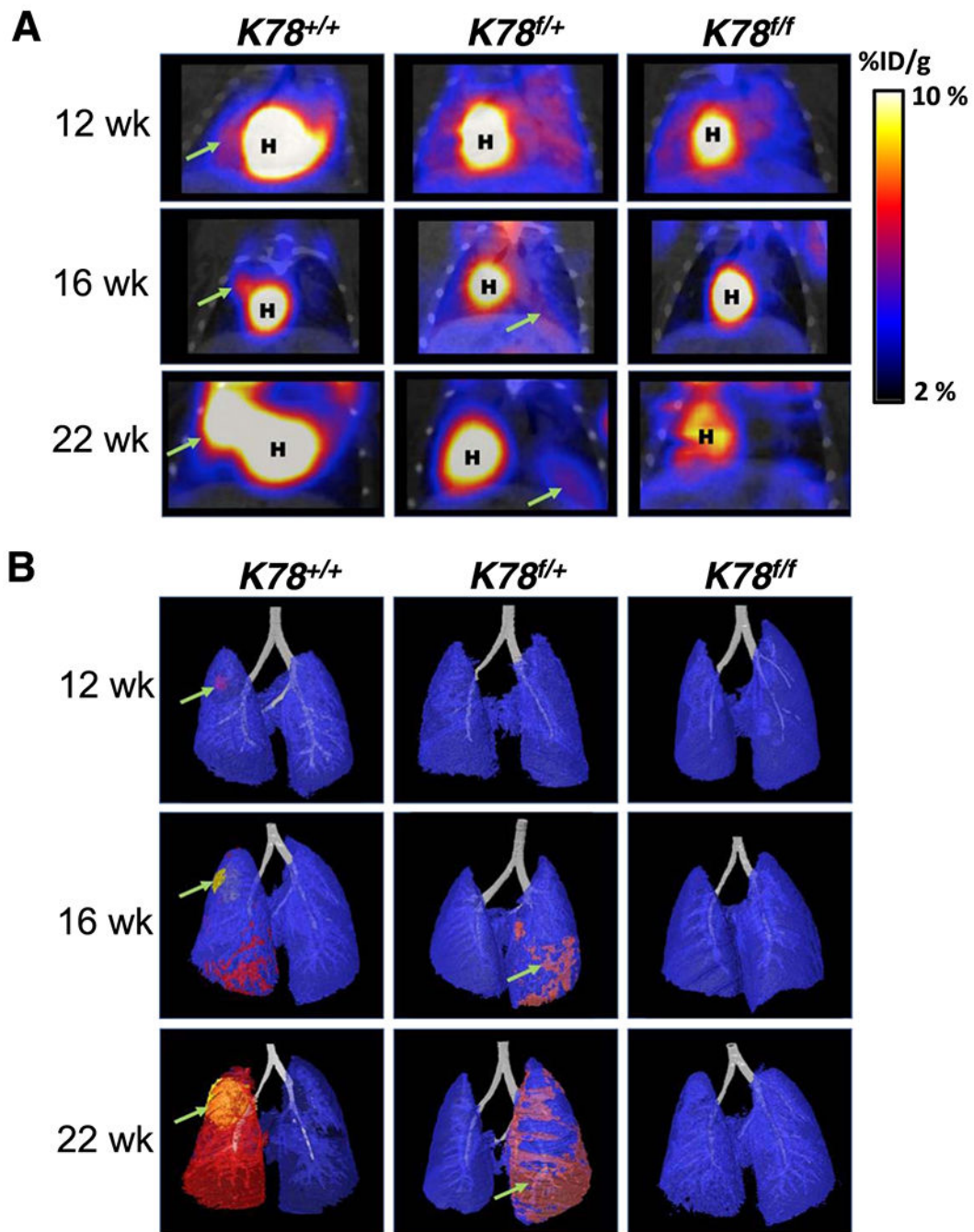


Fig. 3. Imaging of *K78^{+/+}*, *K78^{f/+}*, *K78^{f/f}* mouse lungs.

a FDG PET/CT scan of *K78^{+/+}*, *K78^{f/+}*, *K78^{f/f}* mice for the respective genotype at 12, 16, and 22 wk post adenovirus-Cre intubation. Scans denote the heart (H) and tumorigenic areas (green arrow). On right is the color gradient representing injected dose per gram (% ID/g). **b** Three dimensional contrast-enhanced CT images of lungs of *K78^{+/+}*, *K78^{f/+}* and *K78^{f/f}* mice from (a). Tumorigenic progression (green arrow) from corroborated ^{18}F -FDG PET/CT signal was segmented as pink, red, and yellow to indicate respectively increasing ^{18}F -FDG avidity in the same mouse.

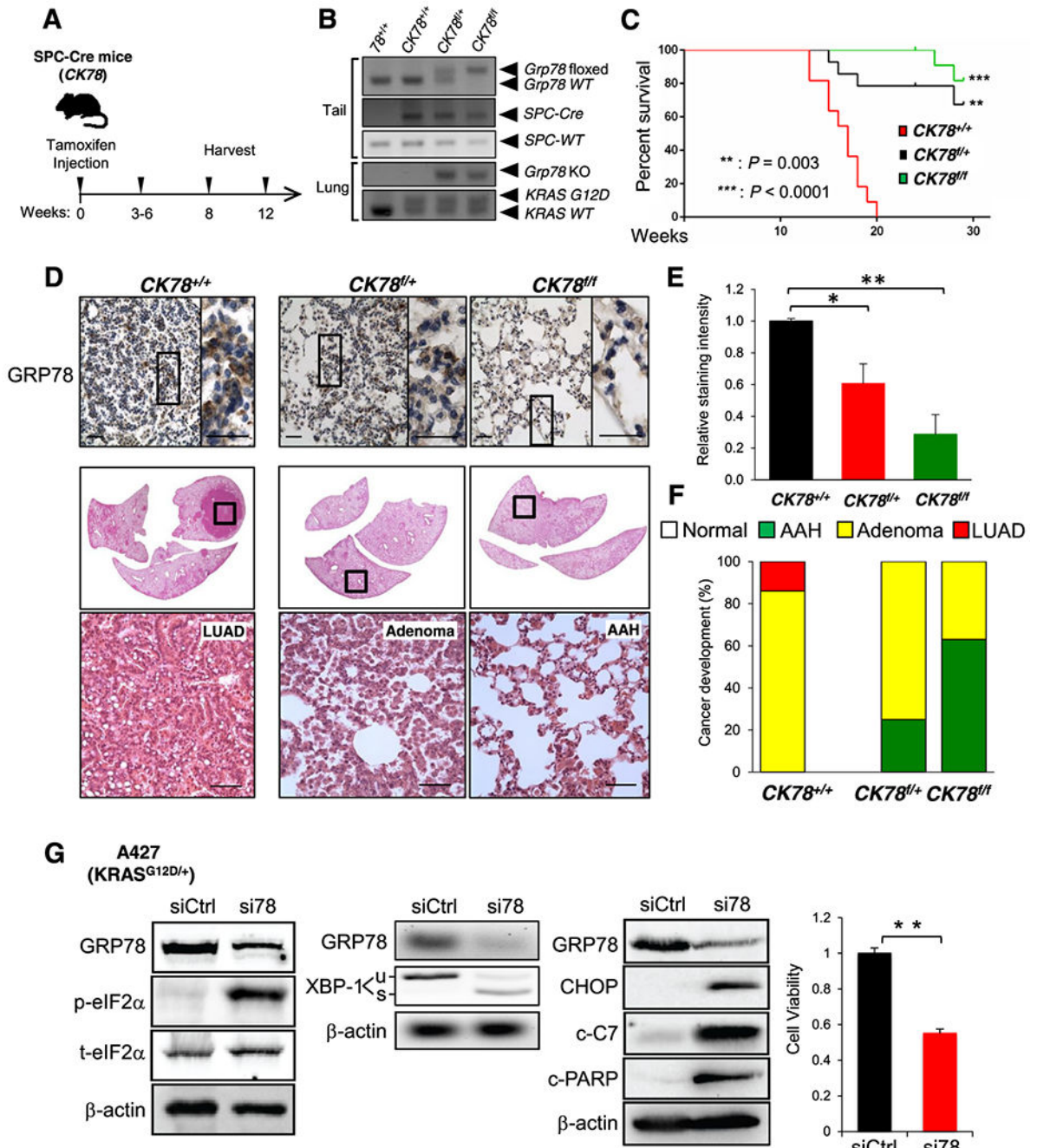


Fig. 4. Analysis and characterization of CK78^{+/+}, CK78^{f/+} and CK78^{f/f} mice following SPC-Cre activation and effect of GRP78 knockdown in a human lung cancer cell line.
a Harvesting schedule for the SPC-Cre, floxed *Grp78* mouse cohorts. To induce the SPC-Cre-recombinase, 10 wk old mice were subjected to intraperitoneal (i.p.) tamoxifen injection and the mouse lungs were harvested at the indicated time points. **b** Representative genotyping results of the SPC-Cre mice using DNA extracted from tail (top three panels) and from lung (bottom two panels) after Cre activation. **c** Kaplan-Meier survival curves of CK78^{+/+} (n=11), CK78^{f/+} (n=11) and CK78^{f/f} (n=13) mice. Male and female mice were

combined as there were no differences between the two groups. *CK78^{fl/+}* and *CK78^{fl/f}* mice exhibited prolonged survival compared to *CK78^{+/+}* mice (**: $p=0.003$) and (***: $p<0.0001$), one-sided log-rank test, respectively. **d** Immunohistochemistry (IHC) staining of GRP78 in lungs of *CK78^{+/+}* mice at 8 wk post-tamoxifen i.p. injection. (Scale bar: 100 μm). Enlarged view of the boxed area is shown to the right. (Scale bar: 100 μm). Below is a cross section of the whole lungs with magnified boxed area showing H&E staining of lung adenocarcinoma (LUAD) lesions. (Scale bar: 200 μm). Lungs of *CK78^{fl/+}* and *CK78^{fl/f}* mice at 12 wk post-tamoxifen injection are also represented. Representative H&E staining images are shown below with examples of adenoma and atypical adenomatous hyperplasia (AAH) lesions in the *CK78^{fl/+}* and *CK78^{fl/f}* lungs respectively. **e** Quantitation of GRP78 staining from (d). The values represent the average staining of the sampled area \pm s.e., * $p<0.05$ and ** $p<0.01$. Number of images that were randomly chosen to be quantified are the following *CK78^{+/+}* (n=10), *CK78^{fl/+}* (n=10) and *CK78^{fl/f}* (n=10). At least three to four mice were analyzed per genotype. **f** Quantitation of the histological grades exhibiting normal morphology (N), AAH, adenoma, or LEI AD of lungs of *CK78^{+/+}* mice at 8 wk and *CK78^{fl/+}* and *CK78^{fl/f}* mice at 12 wk post-tamoxifen i.p. injection. The number of mice analyzed is as follows: *CK78^{+/+}* (n=7), *CK78^{fl/+}* (n=4) and *CK78^{fl/f}* (n=8). **g** A427 cells were transfected with control siRNA (siCtrl) or siRNA specifically targeting GRP78 (si78) for 48 hr and analyzed for levels of phospho (p) and total (t) eIF2 α , unspliced (u) and spliced (s) form of *XBP-1* mRNA, in parallel with *GRP78* and *β -actin* mRNA, CHOP and cleaved form of Caspase-7 (c-C7) and PARP (c-PARP) as well as cell viability measured by WST-1 assay.